https://doi.org/10.5194/tc-2020-241
Preprint. Discussion started: 25 September 2020

The Cryosphere Discussions

Thermal legacy of a large paleolake in Taylor Valley, East Antarctica as evidenced by an airborne electromagnetic survey

Krista F. Myers[1], Peter T. Doran[1], Slawek M. Tulaczyk[2], Neil T. Foley[2], Thue S. Bording[3], Esben Auken[3], Hilary A. Dugan[4], Jill A. Mikucki[5], Nikolaj Foged[3], Denys Grombacher[3], and Ross A. Virginia[6]

[1]Department of Geology and Geophysics, Louisiana State University, Baton Rouge, LA 70803, USA
[2]Department of Earth and Planetary Sciences, University of California Santa Cruz, Santa Cruz, CA 95064, USA
[3]Department of Geoscience, Aarhus University, Aarhus, Denmark
[4]Center for Limnology, University of Wisconsin-Madison, Madison, WI 53706, USA
[5]Department of Microbiology, University of Tennessee, Knoxville, Knoxville, TN 37996, USA
[6]Environmental Studies, Dartmouth College, Hanover, NH 03755, USA

Correspondence to: Krista F. Myers (kristafmyers@gmail.com)

Abstract. Previous studies of the lakes of the McMurdo Dry Valleys have attempted to constrain lake level history, and results suggest the lakes have undergone hundreds of meters of lake level change within the last 20,000 years. Past studies have utilized the interpretation of geologic deposits, lake chemistry, and ice sheet history to deduce lake level history, however a substantial amount of disagreement remains between the findings, indicating a need for further investigation using new techniques. This study utilizes a regional airborne resistivity survey to provide novel insight into the paleohydrology of the region. Mean resistivity maps revealed an extensive brine beneath the Lake Fryxell basin which is interpreted as a legacy groundwater signal from higher lake levels in the past. Resistivity data suggests that active permafrost formation has been ongoing since the onset of lake drainage, and that as recently as 1,000 – 1,500 yr BP, lake levels were over 60 m higher than present. This coincides with a warmer than modern paleoclimate throughout the Holocene inferred by the nearby Taylor Dome ice core record. Our results indicate mid to late Holocene lake level high stands which runs counter to previous research finding a colder and drier era with little hydrologic activity throughout the last 5,000 years.

1 Introduction

Lakes provide a refuge to life in some of the more extreme environments on Earth, especially in places with strong seasonality such as polar regions. Lakes are a relatively stable source of liquid water which can determine the ecological viability of a system (Gooseff et al., 2017). The evolution of lake basins is important to survival of local ecosystems, and interpreting the history of lake levels and water availability can provide important insights into long-term ecosystem dynamics. Despite extremely low temperatures and minimal precipitation, the McMurdo Dry Valleys (MDVs – Fig. 1) are the site of a series of closed basin lakes fed by alpine glacial and snow melt via ephemeral streams as well as by direct subsurface recharge (Toner et al., 2017; Lawrence et al., 2020). Annual lake levels in the MDVs have been recorded since the 1970s which provide a window into the dynamic climatic and geologic drivers of the MDV hydrologic system (Fountain et al., 2016). Lake levels have overall risen since the beginning of observational records starting in 1903 during Robert Scott's first expedition (Scott, 1905), however periods of lake level stagnation as well as lake level drop have also been recorded (Fountain et al., 2016). The fluctuation of the MDV lakes alters the biological and chemical exchange between surface waters, soils, and groundwater,

https://doi.org/10.5194/tc-2020-241
Preprint. Discussion started: 25 September 2020


The Cryosphere Discussions

making it critical for understanding MDV connectivity and ecosystem evolution (Doran et al., 2002; Gooseff et al., 2017; Foley et al., 2019).

The drivers of MDV lake level change represent a complex combination of climate, ice sheet extent, and basin hypsometry. During the Last Glacial Maximum (LGM) roughly 28.5–12.8 ka before present (BP) Antarctica underwent a period of ice sheet thickening and advance (Hall et al., 2015). Stable isotope records from Taylor Dome (located roughly 100 km west of the MDVs) indicate mean annual air temperatures ca. 4-9 °C lower than modern during the LGM (Steig et al., 2000) (Fig. 2). Ice from the East and West Antarctic ice sheets was grounded within the Ross Sea extending to the edge of the continental shelf, roughly 500 km further than the modern-day grounding line (Anderson et al., 2014). During the LGM, grounded ice from the Ross Ice Shelf (RIS) flowed inland, spilled into the ice-free MDVs, and formed an ice dam that reached approximately 350 meters above sea level (masl) (Denton and Marchant, 2000). The grounded RIS in the mouth of Taylor Valley would have allowed for lake levels to reach elevations that would otherwise not be possible (~300–350 masl), forming a massive glacially dammed lake known as Glacial Lake Washburn (GLW), which would have filled all of Taylor Valley (Fig. 3a). The RIS remained grounded at a maximum equilibrium extent along the eastern side of the Transantarctic Mountains until roughly 12,700 ^{14}C yr BP according to Hall and Denton (2000). The grounded ice sheet was completely gone from the mouth of TV sometime between 7,800 to 6,000 yr BP (Cunningham et al., 1999; Hall et al., 2006; Hall et al., 2013; Anderson et al., 2016), leading to the removal of the ice dam in the mouth of TV, which would have resulted in drainage of GLW, and subsequent lake levels would be limited by the 78-81 masl topographic constraint (outflow sill) at Coral Ridge (Fig. 3b). Between 12,000–6,000 yr BP, Taylor Dome ice core record indicates that regional temperatures were up to 5 °C warmer than modern conditions (Fig. 2) (Steig et al., 2000).

Much of the past lake level chronology in Taylor Valley has been established by dating paleodeltas, which form where streams enter the lake and deposit sediment. Previous studies have utilized radiocarbon dating of algal mats within these deltas (Hall and Denton, 2000) and optically stimulated luminescence (OSL) dating of quartz grains (Berger et al., 2013) to constrain the age of the paleodeltas. Hall and Denton (2000) postulate that a large lake occupied the full TV, reaching an elevation of up to 350 masl, between a period of 8,340 to 23,800 yr BP, suggesting lake levels dropped below modern levels by 8 ka BP (Fig. 4). An atmospheric correction was applied to the ^{14}C ages from Hall and Denton (2000) shown in Fig. 4 using the CALIB program (Stuiver et al., 2018). Berger et al. (2013) determined that delta deposits are systematically younger than the ^{14}C dates at comparable elevations by ~5,000 yr (Fig. 4). Other studies (Horsman, 2007; Arcone et al., 2008; Toner et al., 2013) suggested that GLW was much smaller, and only occupied western TV in the Lake Bonney basin. The disagreement of spatial distribution and timing of paleolakes in TV highlights the need to further constrain lake level history. Additionally, a lack of samples yielding ages in the late Holocene for both ^{14}C and OSL samples has led to the assumption that lake levels have remained near or below modern elevations for the last 5,000 yr (Hall and Denton, 2000; Berger et al., 2013). This study provides a third

https://doi.org/10.5194/tc-2020-241
Preprint. Discussion started: 25 September 2020

method for estimating lake level history during the previously unconstrained mid to late Holocene (5 ka to present) using a novel application of electrical resistivity data to identify the subsurface thermal legacy of paleo lake levels in TV.

2 Site Description and Field Campaign

The MDVs are located within the Transantarctic Mountains and make up the largest ice-free region in Antarctica (Levy, 2013). Mean annual valley bottom temperatures in TV range from -14.7 °C to -23.0 °C (Obryk et al., 2020) and the region receives between 3–50 mm water equivalent of precipitation per year (Fountain et al., 2010). Lakes in the MDVs have 3–5 m thick perennial ice covers and vary in volume, chemistry, and biological activity (Lyons et al., 2000). During the austral summer, a short melt window occurs between December to February which accounts for most of the stream input to the lakes (Chinn, 1987). Open water moats form around the perimeter of the lakes during the summer, and water loss occurs due to sublimation of lake ice and evaporation of open water (Dugan et al., 2013; Obryk et al., 2017).

Lake Fryxell, located in TV, is one of the largest lakes in the MDVs at roughly 5.5 km long, 1.75 km wide and 22 m deep (Fig. 1). Lake level measurements show that from 1972 to 2020, Lake Fryxell has undergone ~2.61 m of total lake level rise as measured by manual lake level surveys, at an average rate of ~5.4 cm yr^{-1} (Fig. 5) (Doran and Gooseff, 2020). The lake level record is characterized by high interannual variability in both lake level change (magnitude) and direction (rise versus fall) (Fountain et al., 2016).

2.1 Resistivity Surveys

SkyTEM, a time-domain airborne electromagnetic (AEM) sensor system, was flown over TV in 2011 (see Mikucki et al., 2015 for TV flight lines). The measurement involves pulsing a strong current in a transmitter coil suspended beneath a helicopter. When these currents are turned off rapidly, a primary magnetic field propagates throughout the subsurface, which induces eddy currents in the subsurface at depth. The decay of these eddy currents in turn generates a secondary magnetic field, the strength and time-dependence of which is measured inductively by a receiver coil that is also suspended beneath the helicopter (Foley et al., 2016). The resulting data, which consists of time derivatives of the secondary magnetic field, is used to estimate the resistivity in the subsurface (Ward and Hohmann, 1988). Data collection occurs while the helicopter flies at speeds up to approximately 100 km h^{-1}. The 2011 AEM survey collected 560 km of resistivity data in eastern TV. Flight lines were approximately 500 m apart, and nodes (individual sounding points) were collected every ~25 m along each flight line. For more details and in-depth discussion behind SkyTEM methodology and data collection, see Sørensen and Auken (2004), Mikucki et al. (2015), and Foley et al. (2016).

Specialized inversion software, called Workbench, developed at Aarhus University, was used to process raw resistivity data and invert for layer models of subsurface resistivity (Foley et al., 2016). Mean resistivity maps, which illustrate the mean

https://doi.org/10.5194/tc-2020-241
Preprint. Discussion started: 25 September 2020

resistivity of the subsurface at fixed elevation intervals, were generated in Workbench using a spatially constrained ('quasi-3D') inversion of the data collected from Fryxell basin in 2011 (Viezzoli et al., 2008). These maps are valuable for illustrating lateral continuity and extent of resistivity structures at depth. Five-meter-thick slices of constant elevation from 250 masl to -300 masl were interpolated to generate mean resistivity maps using a 1,000 m search radius and kriging interpolation. Mean resistivity maps were imported into ArcGIS and then overlaid on digital elevation models (Fountain et al., 2017) and high resolution Digital Globe satellite imagery (WorldView 3, provided by the Polar Geospatial Center) to visualize the location and extent of low resistivity regions. The depth of investigation (DOI) was determined in Workbench and represents the maximum depth of reliable resistivity models. Regions of low resistivity (<1,000 Ωm, typical of lake water and brine saturated sediments) have lower DOIs (<100 m) due to signal attenuation in conductive materials, whereas regions of high resistivity (>1,000 Ωm, typical of permafrost and bedrock), have greater DOIs (>300 m) because the EM signal penetrates deeper with less attenuation in these conditions (Christiansen and Auken, 2012; Mikucki et al., 2015; Foley et al., 2016).

Subsurface characteristics and chemistry can be inferred from the relationship of bulk resistivity to temperature, salinity, and liquid volume fraction (Mikucki et al., 2015). The regions of low resistivity underlying higher resistivities are interpreted as liquid brine saturated sediments capped by permafrost and represent the liquid groundwater extent in Fryxell basin. To calculate the thickness of the confining permafrost above this briny aquifer, we performed a search from the surface to the first instance at depth of resistivity values at or below a threshold value of 100 Ωm. The 100 Ωm threshold broadly distinguishes between "dry" or hard-frozen permafrost (above 100 Ωm) and aquifrost or unfrozen ground with a significant liquid fraction in pore spaces (Mikucki et al., 2015; Foley et al., 2016). This is in rough agreement with resistivity values of saturated sediment first explored in the 1970s as part of the DVDP (McGinnis and Jensen, 1971).

Workbench was used to export location, elevation, and depth to brine for each node point of resistivity data collected. Depth to brine values for each node were interpolated to map distribution of the permafrost/brine boundary. Depth to brine maps were smoothed using a low pass filter in ArcGIS to reduce noise, which was particularly high around the edges where data density was lower and signal-to-noise ratios were less favorable.

2.2 Modelling permafrost thickness and age

Permafrost thickness, which is taken as the depth to 100 Ωm boundary, was used to calculate time since initiation of permafrost freeze-back resulting from lake drainage. We adapted Eq. (5) from Osterkamp and Burn (2003);

$$t = s\frac{d^2 \cdot H_s}{2k_b \cdot (-T_{ps})} \qquad \text{Eq. (1)}$$

https://doi.org/10.5194/tc-2020-241
Preprint. Discussion started: 25 September 2020


The Cryosphere Discussions

where t is the age of permafrost in years, s is a conversion factor from seconds to years, d is the thickness of permafrost (m), H_s is the volumetric latent heat of fusion for sediments corrected for porosity in Joules per cubic meter (Jm^{-3}), k_b is the bulk thermal conductivity of permafrost in watts per meter per Kelvin ($Wm^{-1}K^{-1}$), and T_{ps} is the temperature difference between the atmosphere and permafrost freezing front (K). The average air temperature of Lake Fryxell is -20 °C (Obryk et al., 2020), and freezing temperature of brine saturated sediments is between –5 °C to -10 °C (Foley et al., 2016). Here we use an average brine freezing temperature of -5 °C, and a max brine freezing temperature of -8 °C. Therefore, the average T_{ps} is -15 K and maximum T_{ps} is -12 K. The volumetric latent heat of fusion for sediments corrected for porosity is estimated using Eq. (2);

$$H_s = H_v \cdot \varphi \cdot (1 - \varphi_a) \qquad \text{Eq. (2)}$$

where H_s is the volumetric latent heat of the sediments, H_v is the volumetric latent heat of water (334 MJ m^{-3}), ϕ is the porosity of the sediment, and ϕ_a is the fraction of air in pore space. Bulk thermal conductivity of permafrost (k_b) is estimated using Eq. (3);

$$k_b = {k_m}^{1-\varphi} \cdot {k_f}^{\varphi(1-\varphi_a)} \cdot {k_a}^{\varphi \cdot \varphi_a} \qquad \text{Eq. (3)}$$

where k_m is the thermal conductivity of the matrix (Pringle, 2004), k_f is the thermal conductivity of the fluid (Engineering Toolbox, 2004), and k_a is the thermal conductivity of air (Engineering Toolbox, 2009). All thermal conductivity terms are in units of W m^{-1} K^{-1} and values are summarized in Table 1.

To calculate a range of possible permafrost ages for each elevation, a Monte Carlo statistical analysis was performed. Each input variable was assigned a variance (standard deviation). ϕ, ϕ_a, T_{ps}, and k_m were assigned a standard deviation of 20%, and k_f and k_a were assigned a standard deviation of 2% as they are better constrained. We then draw 10,000 realisations, where each input variable is drawn from a normal distribution with mean value and standard deviation as listed in Table 1. For each realisation we calculate permafrost age assuming completely saturated sediment ($\phi_a = 0$) as well as partially saturated sediment. This approach assumes a normal distribution of all parameters, and a homogeneous substrate in both space and time for simplification purposes.

To produce a deterministic upper bound of permafrost ages, Eq. (1) was calculated using the maximum or minimum possible value within one standard deviation for each input variable. H_s was maximized by assigning a maximum ϕ (adding one standard deviation), with and without air in the pore space. Minimum k_b was calculated by minimizing k_m by subtracting one standard deviation and maximizing ϕ by adding one standard deviation, with and without air in pore space. T_{ps} was minimized by adding one standard deviation from the average value (Table 1).

https://doi.org/10.5194/tc-2020-241
Preprint. Discussion started: 25 September 2020


The Cryosphere Discussions

3 Results

Airborne resistivity data were used to map groundwater and permafrost extent within Fryxell basin. A large low resistivity region (<100 Ωm) extends hundreds of meters away from the modern lake extent (Fig. 6). In addition to mapping groundwater, higher resistivities overlaying low resistivity brine in the valley floor are interpreted as regions of permafrost which range from ~5 m thick around the lake edge to over 200 m thick higher up on the valley walls (Fig. 7). Permafrost is thinnest near the modern lake edge and increases in thickness with increasing distance from the lake edge (Fig. 8). Permafrost thickness frequency displays a bimodal distribution, with one mode <50 m thick (near lake edge) and another peak around 150 to 200 m which occurred further up the valley walls (Fig. 9). Permafrost resistivity varies depending on water content and temperature. Confining permafrost generally had values above 10,000 Ωm, which was only observed in some regions of Fryxell basin (Mikucki et al., 2015, McGinnis and Jensen, 1971). A lower resistivity permafrost layer (between 100 to 1,000 Ωm) extends from the brine layer to approximately 81 masl (Fig. 7).

Calculated permafrost ages are plotted against ranges of possible porosity, bulk thermal conductivity, and temperature differences (Fig. 10). The effect of a partially saturated versus fully saturated substrate on the volumetric latent heat of fusion for sediments corrected for porosity (H_s) and bulk thermal conductivity (k_b) was also investigated (Fig. 10). We assumed partially saturated conditions to yield the oldest possible permafrost ages, however we recognize that assuming a homogeneous partially saturated substrate at this permafrost/brine boundary is an oversimplification.

Lower depth to brine values (thinner permafrost) found at low elevations (<80 masl) yielded a smaller range in possible ages. A wide range of calculated ages is seen at higher elevations (>80 masl), and therefore the deeper/older permafrost ages are less constrained (Fig. 11). Maximum permafrost ages for partially saturated conditions (0.24 air fraction in pore space) yielded slightly older ages compared to the first order calculation using average inputs and fully saturated conditions, resulting in a ~500-year increase in age (approximately 1.5 to 1 ka BP) for shallow brines between “average” and “maximum” results (Fig. 11). Figure 12 shows the range of possible ages for a discrete depth to brine (permafrost thickness) of 50 m, 140 m, and 200 m as calculated from the Monte Carlo analysis for both partially saturated and fully saturated conditions. The age uncertainty is smallest for shallower brines (thinner permafrost) compared to deeper brines (thicker permafrost) (Fig. 12). The middle panel of Fig. 12 shows the age probability distribution for 140 m thick permafrost, which roughly corresponds to the 81 masl sill level.

Permafrost age was mapped (using max value, partially saturated inputs in Table 1) using depth to brine/permafrost boundary and Eq. 1 (Fig. 13). Maximum permafrost age was plotted as a function of sounding point elevation to compare to previously reported ^{14}C and OSL ages at corresponding elevations (Fig. 14). A comparison of all three methods shows that even maximum permafrost age calculations cannot reproduce ^{14}C ages of paleodeltas from Hall and Denton (2000). OSL dates are in rough

https://doi.org/10.5194/tc-2020-241
Preprint. Discussion started: 25 September 2020

agreement with permafrost age calculations, especially for low elevations surrounding the modern lake edge (<30 masl) (Fig. 14).

4 Discussion

In polar regions, ubiquitous permafrost isolates surface water fluxes from deeper groundwater systems by forming a relatively impermeable layer, however the distribution of permafrost is dependent on lake level history. This is because changing lake levels drastically alter the surface thermal boundary condition for permafrost from ca. -20 °C (i.e., the mean annual air temperature, when a given site is not beneath lake level) to around the freezing point of freshwater when it is submerged below lake level (e.g., Lawrence and Hendy, 1985). Airborne resistivity data revealed a low resistivity groundwater signal that extends hundreds of meters away from the modern lake edge of Lake Fryxell. In the MDV, this groundwater system is overlaid by permafrost 0 to 100s of meters thick. We propose that this region of low resistivity beneath higher resistivity permafrost is a relic thaw bulb from higher lake levels of the past. The presence of a large paleolake would have altered the thermal regime of inundated regions, allowing for a broader groundwater connection throughout much of TV. As the lake level dropped to modern levels, the paleo-lake bed was exposed to subfreezing surface temperatures resulting in permafrost growth. Gradual freeze-back of past lake beds following lake level drop (transient talik) has been observed in the Arctic, and permafrost continues to form until steady state conditions are reached (Neill et al., 2020). During the late Holocene, a much larger talik would have existed beneath a larger paleolake, and the thickness of permafrost above this relic talik can be used to calculate time since lake drainage using Eq. (1). This model assumes a constant rate of lake level drop and constant T_{ps} for simplification. Lateral heat flux from modern and ancient lakes is not addressed in this study, however it may be important to understand equilibrium thresholds for this evolving groundwater system.

Permafrost age calculations indicate late Holocene lake level high-stands (up to ~81 masl, 63 m higher than modern Lake Fryxell) roughly 1.5 to 1 ka BP that would have filled both Lake Fryxell and Lake Hoare basins (Fig. 3b). Permafrost ages span a wide range of elevations because the depth to brine boundary only roughly follows surface topography. This is probably an indication of subsurface heterogeneity (bedrock, till, lacustrine sediment, and buried ice distribution) which is also apparent in resistivity maps. Shallower depth to brine values (younger ages) are better constrained compared to older and higher elevation brines as suggested by Monte Carlo statistical analysis and can be used as an estimate of uncertainty (Fig. 11, Fig. 12**)**.

Maximum permafrost age calculations paired with paleotemperature records from Taylor Dome can be used to correlate paleoclimate events with hydrologic responses. Lake levels appear to have been the highest around or after 12 ka BP (OSL date from ~250 masl), the end of a warming period from 15 to 12 ka BP. Lake levels likely remained high from 12 to 8 ka BP and subsequently dropped due to the retreat of the grounded RIS from the mouth of TV, which was completely removed by

https://doi.org/10.5194/tc-2020-241
Preprint. Discussion started: 25 September 2020

~8 ka BP (Hall and Denton, 2000, Hall et al., 2004, Anderson et al., 2016, Spector et al., 2017). After the removal of the ice dam lake levels would not be able to exceed the sill level at Coral Ridge (Fig. 1). We measure sill elevation to be 78 – 81 masl based on the DEM of Fountain et al. (2017). Since channel erosion rates are unknown, we use the present-day bank elevation (81 masl) as the topographic threshold that defines the boundary of the Lake Fryxell watershed. Any additional hydrologic input into Lake Fryxell above this 81 masl level would spill into the McMurdo Sound via the channel that cuts through Coral Ridge (Fig. 1).

With inputs tuned to maximize permafrost ages, it was still not possible to yield ages for lake occupation comparable to those estimated by ^{14}C ages of delta deposits (Hall and Denton, 2000) (Fig. 14). Radiocarbon dating from Hall and Denton (2000) suggests that lake levels above modern levels occurred between 22 to 5 ka BP, and that levels did not exceed modern lake elevation after 5 ka BP. OSL dates (Berger et al., 2013) estimate past lake level high stands existed between 12 – 5 ka BP, and do not suggest recent lake level high stands. Our permafrost age calculations agree more with the OSL chronology (60 to 13,400 yr BP) than the ^{14}C (Fig. 14). However, OSL dating has its limitations. OSL data records the burial age of the quartz grain, which may be different from the deposition age. Rates of past sediment transport and deposition are not currently known, so this lag in deposition versus burial time is unresolved. Secondly, OSL dates are collected from depth, meaning the dates may not be an accurate representation of the most recent occupation of that delta/lake level elevation. Because of these two reasons, it is inherently difficult to determine the exact age that the delta was last occupied. Several studies have shown a substantial radiocarbon reservoir effect in the MDVs, but modern lake edges and streams are well equilibrated with the modern atmosphere, so deltas should not inherent old carbon (e.g. Doran et al. 1999, 2014; Hendy and Hall 2006). However, it may just be that the present is not an appropriate analog for the past in this case. The large glacial lake of the past may have had more ancient unequilibrated carbon associated with it due to melt coming from the ancient RIS, even at the lake edges. If radiocarbon dates in the paleodeltas are reduced just 5 ka, both OSL and ^{14}C estimates agree with a drainage event associated with the removal of the RIS around 8 ka BP when lake levels dropped to or below the 81 masl sill threshold.

Other studies focusing on the paleolimnology of Lake Fryxell basin suggest Holocene draw down events; however, the magnitude and timing of these events are somewhat contradictory. Lyons et al. (1998) calculates that Lake Fryxell desiccated into a small (7 m deep) pond in the late Holocene. The stable isotope record indicates that bottom waters are depleted in $\delta^{18}O$ and δD with depth suggesting loss of ice cover and partial desiccation between 1-4 ka BP followed by refilling around 1 ka BP (Lyons et al., 1998). A partial desiccation event cannot be resolved using either paleodelta age or resistivity data from this study. Paleodeltas would be obscured by modern lake levels, and any permafrost freeze-back signature from drainage would be reset by the modern talik. Another study by Wittaker et al. (2008) used the presence of carbonate layers in sediment cores collected from Lake Fryxell to determine Holocene lake level fluctuations. Carbonate layers are formed during lake drawdown events, which leads to concentration and precipitation of salts. Wittaker et al. (2008) found that these carbonate layers suggest only 4 episodes of significant lake level drawdown (6.4, 4.7, 3.8 and 1.6 ka BP) which would have been no more than 3–4.5

https://doi.org/10.5194/tc-2020-241
Preprint. Discussion started: 25 September 2020

m below modern lake level. Due to conflicting conclusions from past studies, we cannot reliably say if there was a partial desiccation of Lake Fryxell during the Holocene.

Multiple lines of evidence support the maximum permafrost age calculation: 1) Permafrost at approximately 81 masl falls between the 1.5 to 1 ka BP age contours. 2) Taylor Dome ice core records show a highly variable Holocene, with short lived peaks up to + 6 °C above modern temperatures between 1-2 ka BP (Steig et al., 2000). 3) The existence of a large and very well-preserved delta on Crescent Stream in Fryxell basin, with nearly zero slope and sharp transitions between the topset and foreset suggest low degrees of weathering (Fig. 15). Weathering of delta deposits has not been rigorously addressed in previous literature; however, through visual comparison in the field as well as using DEMs and satellite imagery, the delta on Crescent Stream is the best-preserved and best defined delta in Fryxell basin. Because this delta occurs at 81 masl, the maximum possible lake level without grounded ice at the mouth of TV, the delta may have formed through multiple cycles of filling and drainages. Lake Fryxell could have reached 81 masl multiple times in the past, and we suggest that periods with warmer than modern conditions such as the late Holocene could result in this common lake level elevation, and any additional hydrologic input would result in spill over into the McMurdo Sound. The combination of a highly preserved delta deposit at 81 masl, the approximate permafrost age of 1.5 to 1 ka BP, and short lived peaks in temperatures (up to 6 °C warmer than modern) between 1 to 2 ka BP, suggests that it was possible for lake level be at the sill level at some time in the past 2,000 years (Fig. 15).

5 Conclusions

Lake levels in TV have fluctuated in the past, leaving behind a complex history of overprinted lacustrine deposits and subsurface thermal signatures. A novel approach using airborne transient electromagnetic surveys provides new evidence that supports the existence of much higher lake levels in Fryxell basin by constraining lake level timing and extent. This study provides new insight on lake level evolution in TV during the Holocene, a period in which past studies are contradictory and significant gaps remain. Lake levels were higher potentially during and after the LGM when an ice dam blocked the mouth of TV, allowing for lake levels to increase by over 280 m compared to modern level. Taylor Dome ice core records indicate an abrupt warming of >15 °C from 15 – 12 ka BP, (Steig et al., 2000), which may have coincided with the maximum lake level of GLW. Following ice sheet retreat approximately 8 ka BP, GLW drained and lake level likely fluctuated from at or below modern levels (18 masl) up to 81 masl between 8 to 1.5 ka BP. Around 1.5 – 1 ka BP, lake levels were at the 81 masl sill level and have subsequently dropped to or below modern levels.

Short lived changes in temperature such as a 6 °C increase in the late Holocene could have resulted in anywhere between 60 to 80 m of lake level rise and subsequent drawdown. Closed basin MDV lakes are characterized by high variability and extreme sensitivity to both climate and geologic drivers. Modern and paleohydrologic evidence indicates a highly dynamic system in which modest temperature forcings can initiate a large-scale hydrologic response.

https://doi.org/10.5194/tc-2020-241
Preprint. Discussion started: 25 September 2020

Data availability

Lake level data for Fig. 5 is available at https://mcm.lternet.edu/content/lake-level-surveys-mcmurdo-dry-valleys-antarctica-1991-present (Doran and Gooseff, 2020).
SkyTEM data collected in 2011 is available at https://www.usap-dc.org/view/dataset/601071

Author Contributions

KMyers wrote the text, conducted data analysis, and made the figures. PDoran helped write the text as well as develop methods and concepts. STulaczyk and NFoley provided conceptual framework for paper including the method to determine permafrost age from Osterkamp and Burns (2003). EAuken, TBording, NFoged, and DGrombacher provided technical details and support regarding electromagnetic data and processing, as well as edits to the text. TBording also provided help on Monte Carlo simulations. HDugan, JMikucki, and RVirginia all contributed to SkyTEM data collection, conceptual framework for the project, and edits to the text and figures.

Competing Interests

The authors declare they have no conflict of interest.

Acknowledgements

This research is funded by the National Science Foundation (NSF) Grant #OPP-1637708 for Long Term Ecological Research. This material is based upon work supported by the NSF Graduate Research Fellowship under Grant No. 1247192. Support for KM and PD was also provided by the Louisiana State University John Franks Chair Fund. Contributions of ST and NFoley to this work were supported by two grants from NSF, 1344349 and 1644187. Contributions of JM were supported by NSF grant number OPP-1344348. Contributions for RVirginia were supported by NSF grant number 1043618. Other support for this project was provided by NSF grant numbers 1643687, 1643536, and 1643775. Geospatial support for this work provided by the Polar Geospatial Center under NSF-OPP awards 1043681 and 1559691. Any opinions, finding, conclusions, or recommendations expressed in the material are those of the authors and do not necessarily reflect the views of the National Science Foundation.

https://doi.org/10.5194/tc-2020-241
Preprint. Discussion started: 25 September 2020

References

Anderson, J.B., Conway, H., Bart, P.J., Witus, A.E., Greenwood, S.L., McKay, R.M., Hall, B.L., Ackert, R.P., Licht, K., Jakobsson, M., & Stone, J.O. Ross Sea paleo-ice sheet drainage and deglacial history during and since the LGM. Quat. Sci. Rev. 100, 31–54 (2014).

Anderson, J.B., Wilson, G.S., Fink, D., Lilly, K., Levy, R.H., & Townsend, D. Reconciling marine and terrestrial evidence for post LGM ice sheet retreat in southern McMurdo Sound, Antarctica. Quat. Sci. Rev. 157, 1–13 (2016).

Arcone, S.A., Delaney, A.J., Prentice, M.L., & Horsman, J.L. GPR reflection profiles of sedimentary deposits in lower Taylor Valley, Antarctica, paper presented at Twelfth International Conference on Ground Penetrating Radar, Birmingham, United Kingdom, 15–19 June. (2008).

Berger, G. W., Doran, P.T., & Thomsen, K.J. Micro-hole and multigrain quartz luminescence dating of Paleodeltas at Lake Fryxell, McMurdo Dry Valleys (Antarctica), and relevance for lake history. Quat. Geochronol. 18, 119–134 (2013).

Chinn, T.J.H. Accelerated Ablation at a Glacier Ice-Cliff Margin, Dry Valleys, Antarctica. INSTAAR, Univ. Color. 19, 71–80 (1987).

Christiansen, A. V., and E. Auken. A global measure for depth of investigation, Geophysics, 77, 4,WB171-WB177, (2012).

Cunningham, W.L., Leventer, A., Andrews, J.T., Jennings, A.E., & Licht, K.J. Late Pleistocene-Holocene marine conditions in the Ross Sea, Antarctica: Evidence from the diatom record. Holocene 9, 129–139 (1999).

Denton, G.H. & Marchant, D.R. The Geologic Basis for a Reconstruction of a Grounded Ice Sheet in McMurdo Sound, Antarctica, at the Last Glacial Maximum. Geogr. Ann. Ser. A, Phys. Geogr. 82, 167–211 (2000).

Doran, P.T., Berger, G.W., Lyons, W.B., Wharton, R.A., Divisson, M.L., Southon, & J., Dibb, J.E. Dating Quaternary lacustrine sediments in the McMurdo Dry Valleys, Antarctica. Palaeogeogr. Palaeoclimatol. Palaeoecol. 147, 223–239 (1999).

Doran, P.T., McKay, C.P., Clow, G.D., Dana, G.L., Fountain, A.G., Nylen, T., & Lyons, W.B. Valley floor climate observations from the McMurdo dry valleys, Antarctica, 1986-2000. J. Geophys. Res. Atmos. 107, 1–12 (2002).

https://doi.org/10.5194/tc-2020-241
Preprint. Discussion started: 25 September 2020

350 Doran, P.T., & Gooseff, M.N. McMurdo Dry Valleys LTER: Lake level surveys in the McMurdo Dry Valleys, Antarctica from 1991 to present. Environmental Data Initiative. DOI: 10.6073/pasta/3d0e0c4d844792d9964dd4179a3d83aa. (2020) Dataset accessed 16 July 2020.

Dugan, H., Obryk, M. & Doran, P.T. Lake ice ablation rates from permanently ice-covered Antarctic lakes. J. Glaciol. 59,
355 (2013).

Engineering ToolBox, (2004). Ice - Thermal Properties. [online] Available at: https://www.engineeringtoolbox.com/ice-thermal-properties-d_576.html [Accessed February 20, 2020].

360 Engineering ToolBox, (2009). Air - Thermal Conductivity. [online] Available at: https://www.engineeringtoolbox.com/air-properties-viscosity-conductivity-heat-capacity-d_1509.html [Accessed February 20, 2020].

Foley, N. et al. Helicopter-borne transient electromagnetics in high-latitude environments: An application in the McMurdo Dry Valleys, Antarctica. Geophysics 81, WA87-WA99 (2016).
365

Foley, N. et al. Evidence for Pathways of Concentrated Submarine Groundwater Discharge in East Antarctica from Helicopter-Borne Electrical Resistivity Measurements. Hydrology 6, 54 (2019).

Fountain, A.G., Nylen, T.H., Monaghan, A., Basagic, H.J. & Bromwich, D. Snow in the McMurdo Dry Valleys, Antarctica.
370 Int. J. Climatol. 30, 633–642 (2010).

Fountain, A.G. et al. The Impact of a Large-Scale Climate Event on Antarctic Ecosystem Processes. Bioscience 66, 848–863 (2016).

375 Fountain, A.G., Fernandez-Diaz, J.C., Obryk, M., Levy, J., Gooseff, M., Van Horn, D.J., Morin, P., & Shrestha, R. High-resolution elevation mapping of the McMurdo Dry Valleys, Antarctica, and surrounding regions, Earth Syst. Sci. Data, 9, 435-443 (2017).

Gooseff, M.N., Barrett, J.E., Adams, B.J., Doran, P.T., Fountain, A.G., Lyons, W.B., McKnight, D.M., Priscu, J.P., Sokol,
380 E.R., Takacs-Vesbach, C., Vandegehuchte, M.L., Virginia, R.A., and Wall, D.H. Decadal ecosystem response to an anomalous melt season in a polar desert in Antarctica. Nature Ecology and Evolution. 1:1334–1338. (2017).

https://doi.org/10.5194/tc-2020-241
Preprint. Discussion started: 25 September 2020

Hall, B.L. & Denton, G.H. Radiocarbon chronology of Ross Sea drift, eastern Taylor Valley, Antarctica; evidence for a grounded ice sheet in the Ross Sea at the last glacial maximum. Geogr. Ann. Ser. A Phys. Geogr. 82, 305–336 (2000).

Hall, B.L., Baroni, C. & Denton, G.H. Holocene relative sea-level history of the Southern Victoria Land Coast, Antarctica. Glob. Planet. Change 42, 241–263 (2004).

Hall, B.L., Hoelzel, A.R., Baroni, C., Denton, G.H., LeBoeuf, B.J., Overturf, B., and Topf, A.L. Holocene elephant seal distribution implies warmer-than-present climate in the Ross Sea. Proceedings of the National Academy of Sciences. 103, 10213-10217 (2006).

Hall B.L., Denton, G.H., Stone, J.O., and Conway, H. History of the grounded ice sheet in the Ross Sea sector of Antarctica during the Last Glacial Maximum and the last termination. Antarctic palaeoenvironments and earth-surface processes. 381, 167-181 (2013).

Hall, B.L., Denton, G.H., Heath, S.L., Jackson, M.S. & Koffman, T.N.B. Accumulation and marine forcing of ice dynamics in the western Ross Sea during the last deglaciation: Supplementary Info. Nat. Geosci. 8, 625–628 (2015).

Horsman, J.L. The origin of sandy terraces in eastern Taylor Valley, Antarctica, from Ground Penetrating Radar: A test of the Glacial Lake Washburn delta interpretation, MS thesis, 258 pp., Plymouth State University, Plymouth, New Hampshire. (2007).

Lawrence, M.J.F. and Hendy, C.H. Water column and sediment characteristics of Lake Fryxell, Taylor Valley, Antarctica. New Zealand Journal of Geology and Geophysics, 28(3), pp.543-552 (1985).

Lawrence, J.P., Doran, P.T., Winslow, L.A. and Priscu, J.C. Subglacial brine flow and wind-induced internal waves in Lake Bonney, Antarctica. Antarctic Science, 32(3), pp.223-237 (2020).

Levy, J. How big are the McMurdo Dry Valleys? Estimating ice-free area using Landsat image data. Antarct. Sci. 25, 119–120 (2013).

Lyons, W.B., Tyler, S.W., Wharton, R.A., McKnight, D.M. & Vaughn, B.H. A Late Holocene desiccation of Lake Hoare and Lake Fryxell, McMurdo Dry Valleys, Antarctica. Antarct. Sci. 10, 247–256 (1998).

https://doi.org/10.5194/tc-2020-241
Preprint. Discussion started: 25 September 2020

Lyons, W.B., Fountain, A., Doran, P.T., Priscu, J.C., Neumann, K., & Welch, K.A., Importance of landscape position and legacy: The evolution of the lakes in Taylor Valley, Antarctica. Freshw. Biol. 43, 355–367 (2000).

McGinnis, L.D. & Jensen, T.E. Permafrost-Hydrogeologic Regimen in Two Ice-Free Valleys, Antarctica, from Electrical Depth Soundings. 389–409 (1971).

Mikucki, J.A., Auken, E., Tulaczyk, S., Virginia, R.A., Schamper, C., Sorensen, K.I., Doran, P.T., Dugan, H., & Foley, N. Deep groundwater and potential subsurface habitats beneath an Antarctic dry valley. Nat. Commun. 6, 6831 (2015).

Obryk, M.K., Doran, P.T., Waddington, E.D. & McKay, C.P. The influence of föhn winds on Glacial Lake Washburn and palaeotemperatures in the McMurdo Dry Valleys, Antarctica, during the Last Glacial Maximum. Antarct. Sci. 29, 457–467 (2017).

Obryk, M.K., Doran, P.T., Fountain, A.G., Myers, M., McKay, C.P. Climate from the McMurdo Dry Valleys, Antarctica, 1986 – 2017: Surface Air Temperature Trends and Redefined Summer Season. Journal of Geophysical Research: Atmospheres. 125 (2020).

Osterkamp, T.E. & Burn, C.R. Permafrost, in Encyclopedia of Atmospheric Sciences, edited by J. R. Holton, pp. 1717–1729, Academic, Oxford, U.K. (2003).

Sørensen, K. I., and E. Auken. SkyTEM - A new high-resolution helicopter transient electromagnetic system, Exploration Geophysics, 35,191-199, (2004).

Scott, R.F., The Voyage of the 'Discovery', C. Scribner's Sons, New York (1905).

Steig, E.J., Morse, D.L., Waddington, E.D., Stuiver, M., Grootes, P.M., Mayewski, P.A., Twickler, M.S., & Whitlow, S.I. Wisconsinan and Holocene Climate History from an Ice Core at Taylor Dome, Western Ross Embayment, Antarctica. Geogr. Ann. Ser. A Phys. Geogr. 82A, 213–235 (2000).

Stuiver, M., Reimer, P.J., & Reimer, R.W. CALIB 7.1 [WWW program] at http://calib.org, accessed 2018-6-4 (2018).

Toner, J.D., Sletten, R.S. & Prentice, M.L. Soluble salt accumulations in Taylor Valley, Antarctica: Implications for paleolakes and Ross Sea Ice Sheet dynamics. J. Geophys. Res. Earth Surf. 118, 198–215 (2013).

https://doi.org/10.5194/tc-2020-241
Preprint. Discussion started: 25 September 2020

450 Toner, J.D., Catling, D.C. and Sletten, R.S.. The geochemistry of Don Juan Pond: Evidence for a deep groundwater flow system in Wright Valley, Antarctica. Earth and Planetary Science Letters, 474, pp.190-197 (2017).

Viezzoli, A., A. V. Christiansen, E. Auken, and K. I. Sørensen. Quasi-3D modelling of airborne TEM data by Spatially Constrained Inversion, Geophysics, 73, 3,F105-F113, (2008).

455

Ward, S.H. & Hohmann G.W. Electromagnetic theory for geophysical applications, in M. N. Nabighian, ed., Electromagnetic methods in applied geophysics: SEG, 130–311. (1988).

460

https://doi.org/10.5194/tc-2020-241
Preprint. Discussion started: 25 September 2020

465 Fig. 1. Overview map of the McMurdo Dry Valleys. Lake Fryxell is located in the eastern portion of Taylor Valley. Satellite imagery from Landsat Imagery Mosaic Antarctica (LIMA) published 2009.

470

https://doi.org/10.5194/tc-2020-241
Preprint. Discussion started: 25 September 2020

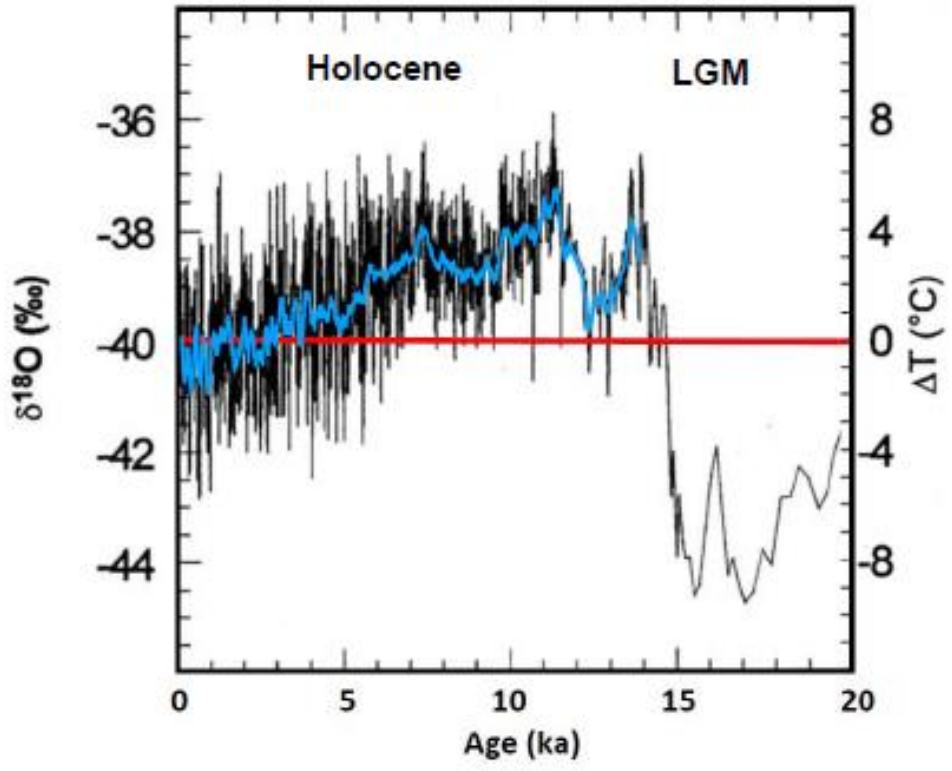

475 Fig. 2. Stable isotope ($\delta^{18}O$) record from Taylor Dome ice core and paleotemperature reconstruction. A reference line for 0 ΔT (°C) is shown in red, representing deviation from modern temperatures. The blue line represents a 100-year running average of the data. Modified from Steig et al. (2000).

480

485

https://doi.org/10.5194/tc-2020-241
Preprint. Discussion started: 25 September 2020

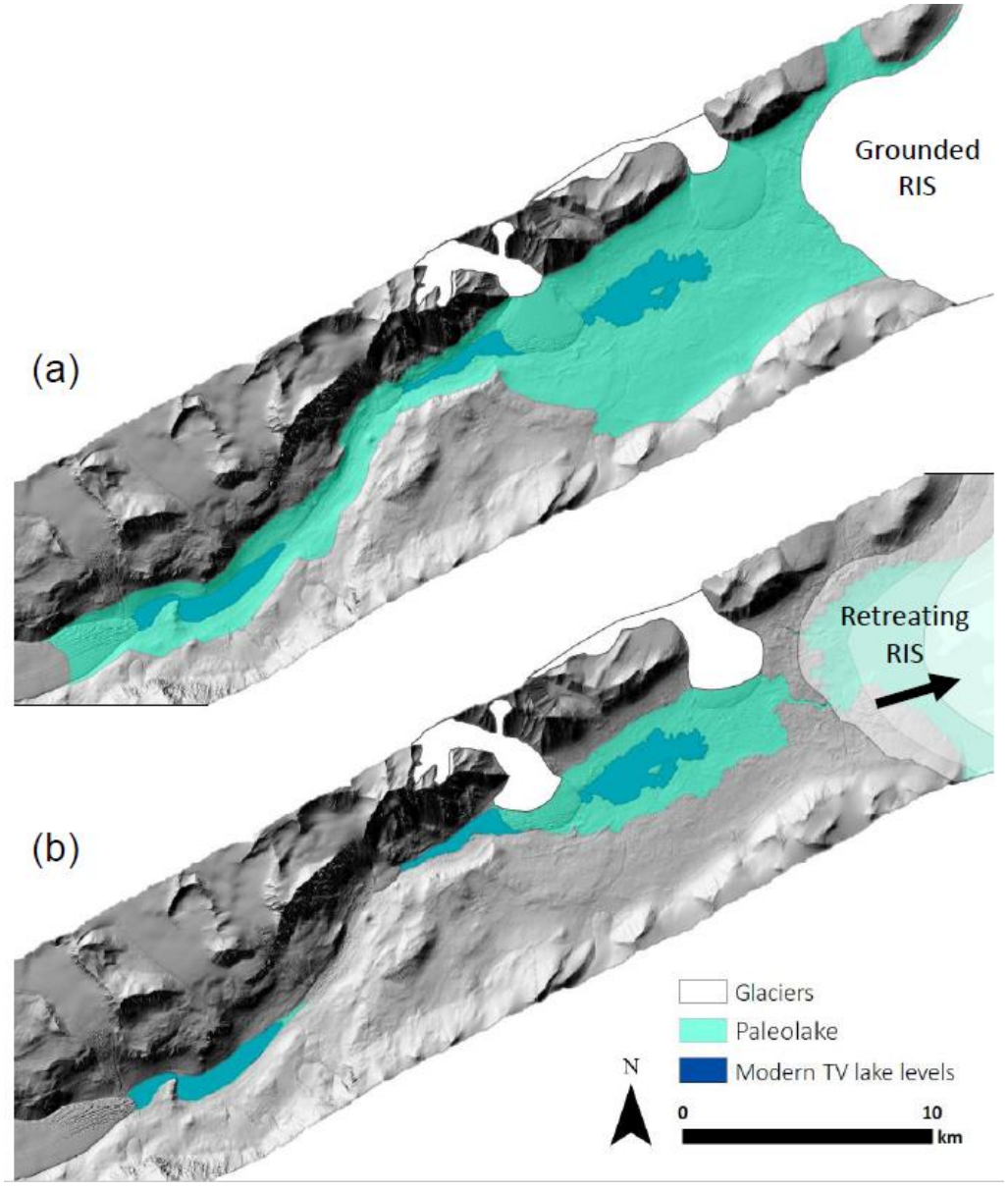

Fig. 3. (a) Glacial Lake Washburn extending up Taylor Valley (300 masl). Extent of grounded Ross Ice Sheet is estimated from maps of Ross Sea Drift moraine locations (Hall and Denton, 2000); (b) Holocene extent of paleolake, limited by 81 masl sill between Lake Fryxell and the McMurdo Sound. Modern day lake levels shown in dark blue. Extent of alpine glaciers (Canada and Commonwealth glaciers in white) are estimated. DEM (1 m resolution) is from 2014-15 LiDAR survey, accessed via OpenTopography (Fountain et al., 2017).

https://doi.org/10.5194/tc-2020-241
Preprint. Discussion started: 25 September 2020

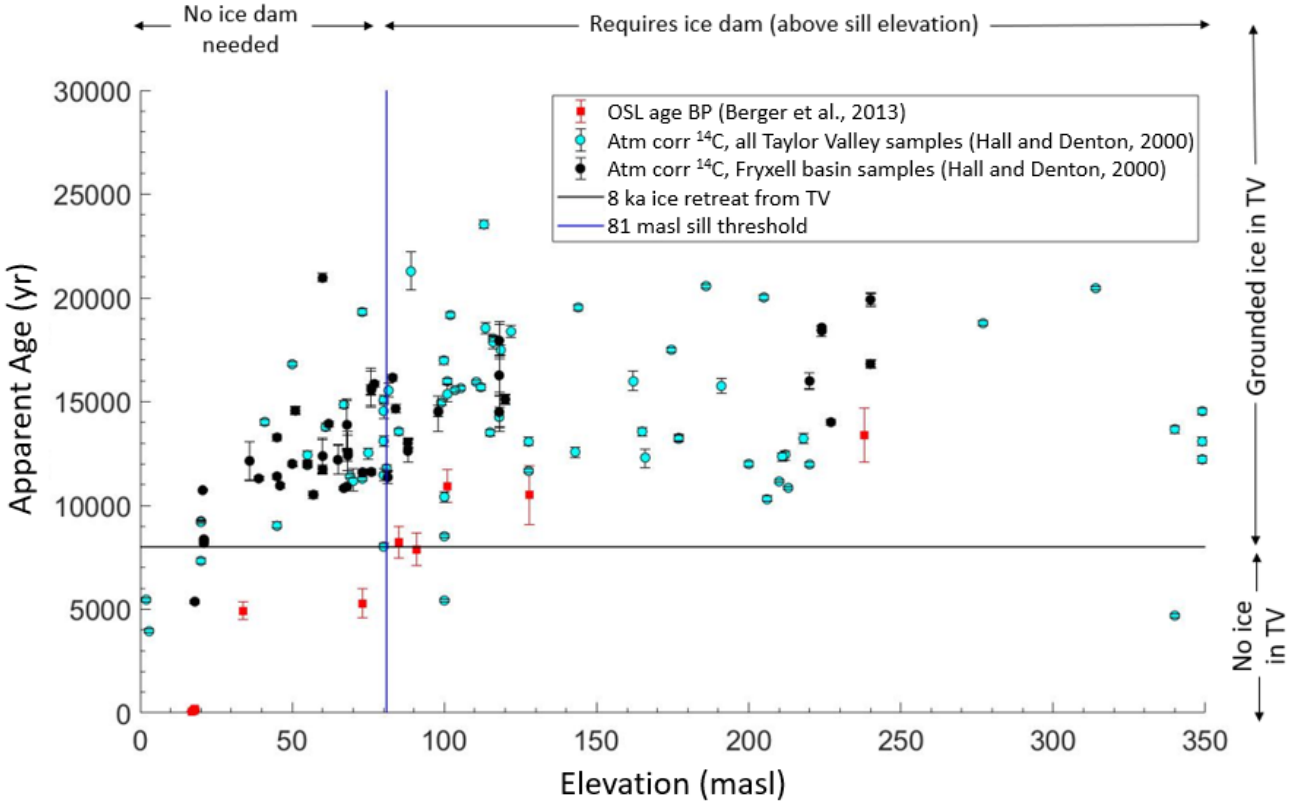

Figure 4. Age of delta deposits from 14C dating of preserved algal mats (Hall and Denton, 2000) shown as circles. Samples from all of Taylor Valley and just Fryxell basin shown as black and cyan circles, respectively. Age estimates using optically stimulated luminescence (OSL) dating shown as red squares (Berger et al., 2013). Black line represents retreat of grounded Ross Ice Sheet from the mouth of Taylor Valley (~8 ka), blue line represents approximate elevation of sill at Coral Ridge (81 masl).

https://doi.org/10.5194/tc-2020-241
Preprint. Discussion started: 25 September 2020

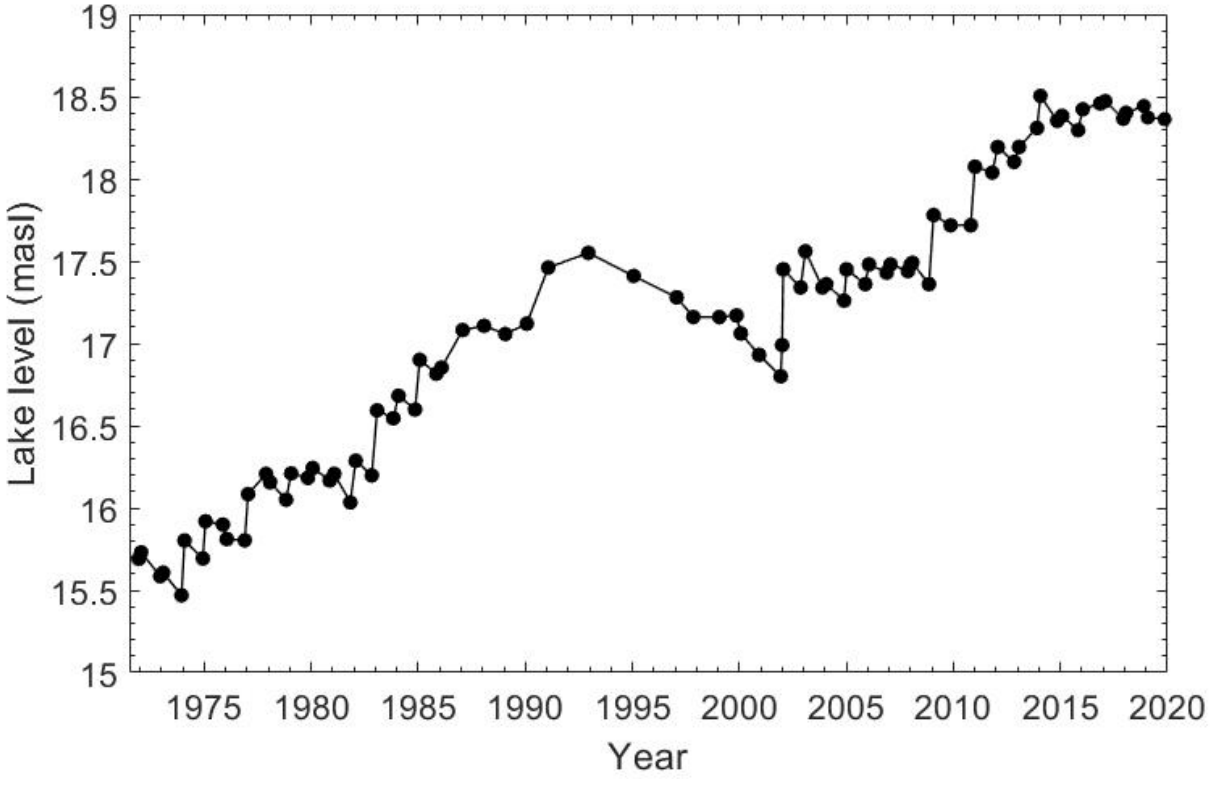

515 Fig. 5. Lake level elevation of Lake Fryxell from 1972 to 2020. Lake levels are determined by manual survey. Data can be accessed at https://mcm.lternet.edu/. (Doran and Gooseff, 2020)

520

525

https://doi.org/10.5194/tc-2020-241
Preprint. Discussion started: 25 September 2020

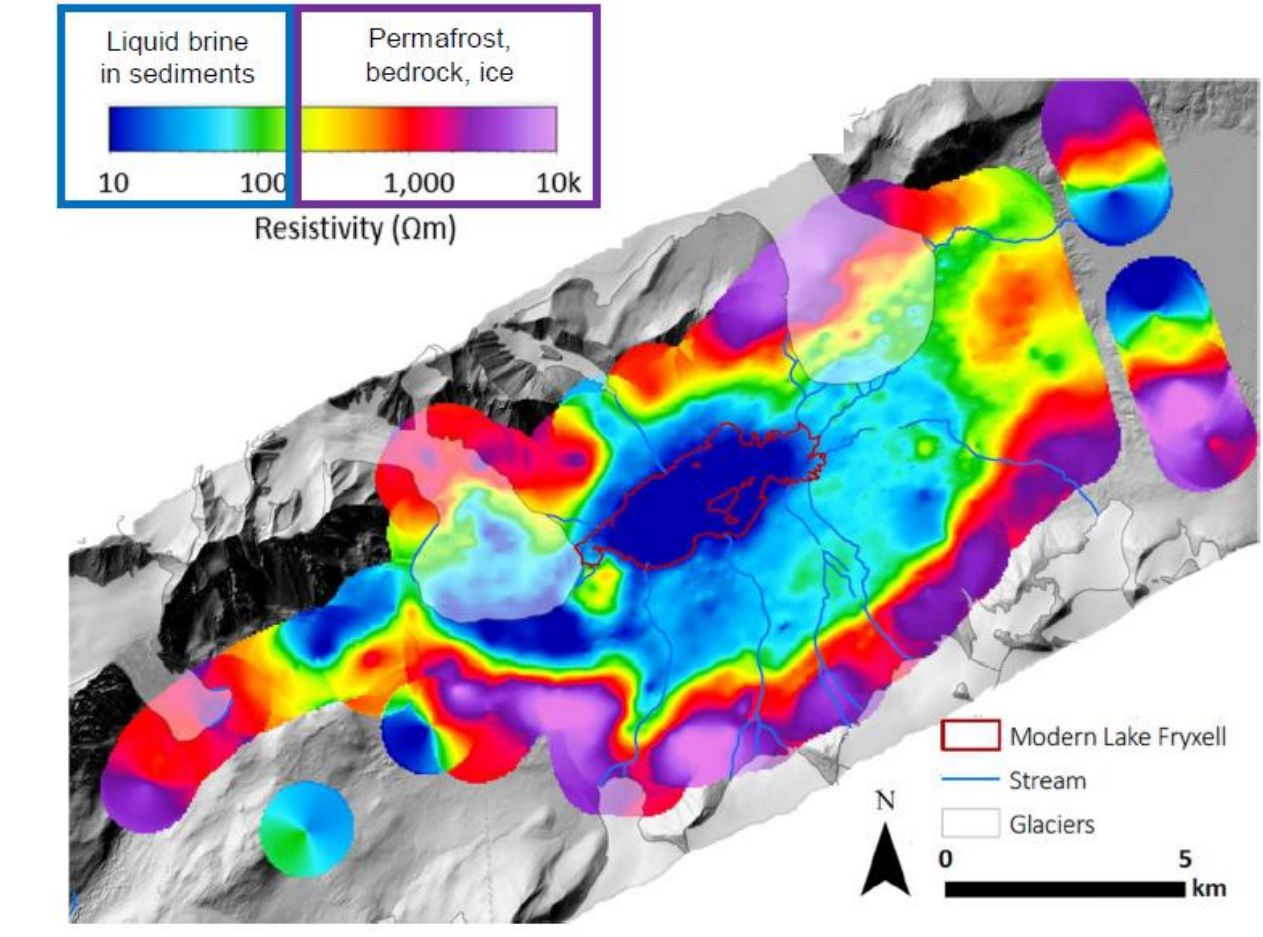

530

Fig. 6. Mean resistivity map of constant elevation (-100 masl, 5 m thick slice) generated from SkyTEM data. Modern lake Fryxell shown in red, streams in blue, and glaciers as transparent polygons. DEM (1 m resolution) is from 2014-15 LiDAR survey, accessed via OpenTopography (Fountain et al., 2017).

535

540

https://doi.org/10.5194/tc-2020-241
Preprint. Discussion started: 25 September 2020

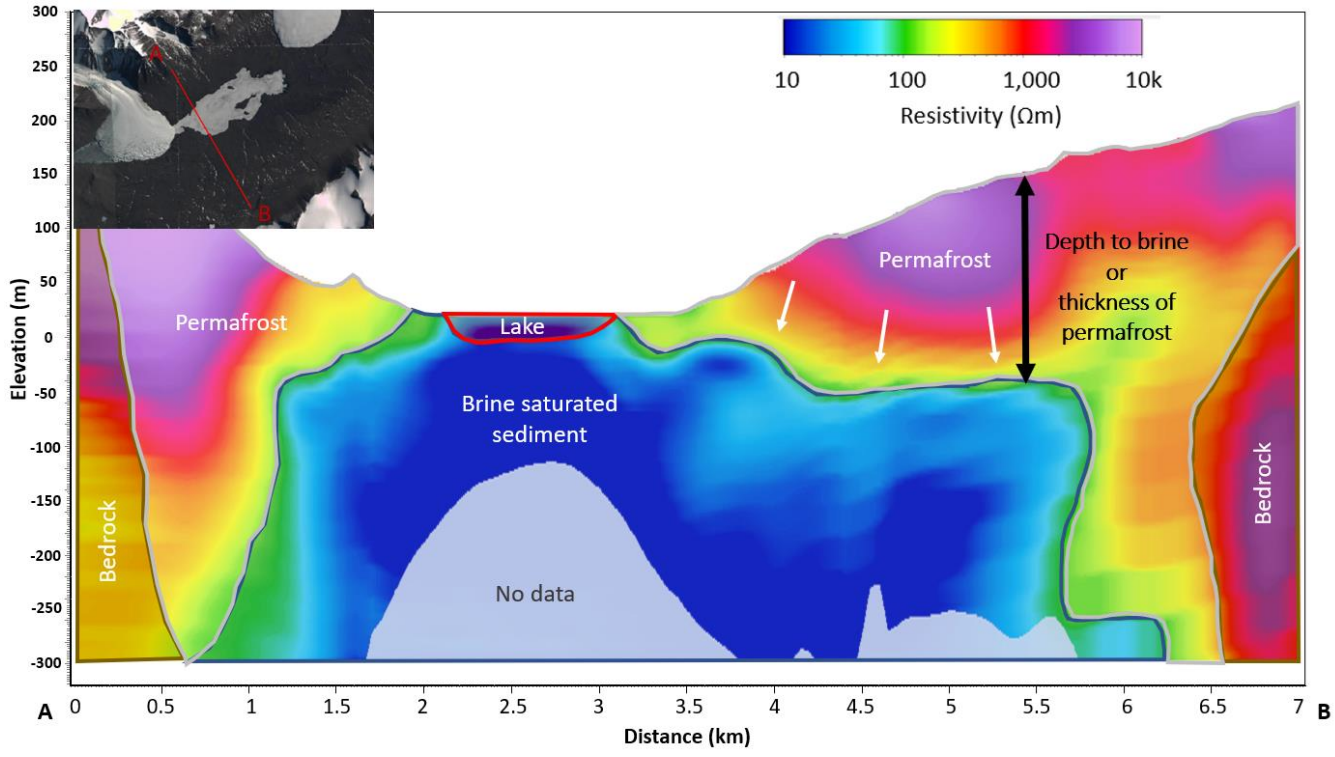

Fig. 7. North-south transect created from 3D grid. Mean resistivity maps created using 1 km search radius (2x line spacing), 5 m elevation slices. Subsurface boundaries are approximated, and interpretations based on Mikucki et al. (2015).

https://doi.org/10.5194/tc-2020-241
Preprint. Discussion started: 25 September 2020

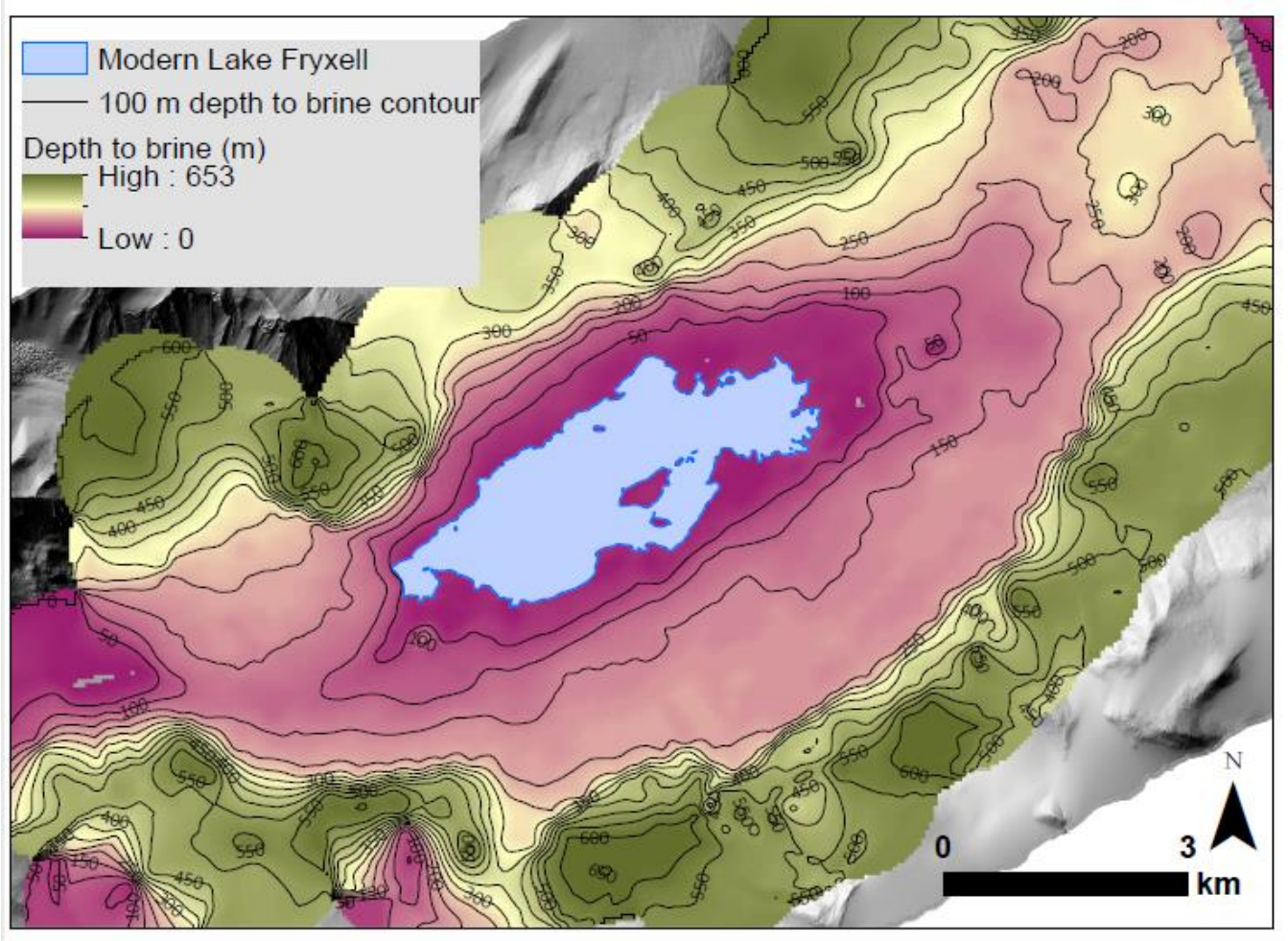

Fig. 8. Map showing depth to 100 Ωm brine/permafrost boundary. Interpolation was smoothed using a low pass filter in ArcGIS to reduce edge noise. Edges (higher elevations and deeper brine layers) are less reliable because of inversion interpolation and limitations of depth of investigation. DEM (1 m resolution) is from 2014-15 LiDAR survey, accessed via OpenTopography (Fountain et al., 2017).

https://doi.org/10.5194/tc-2020-241
Preprint. Discussion started: 25 September 2020

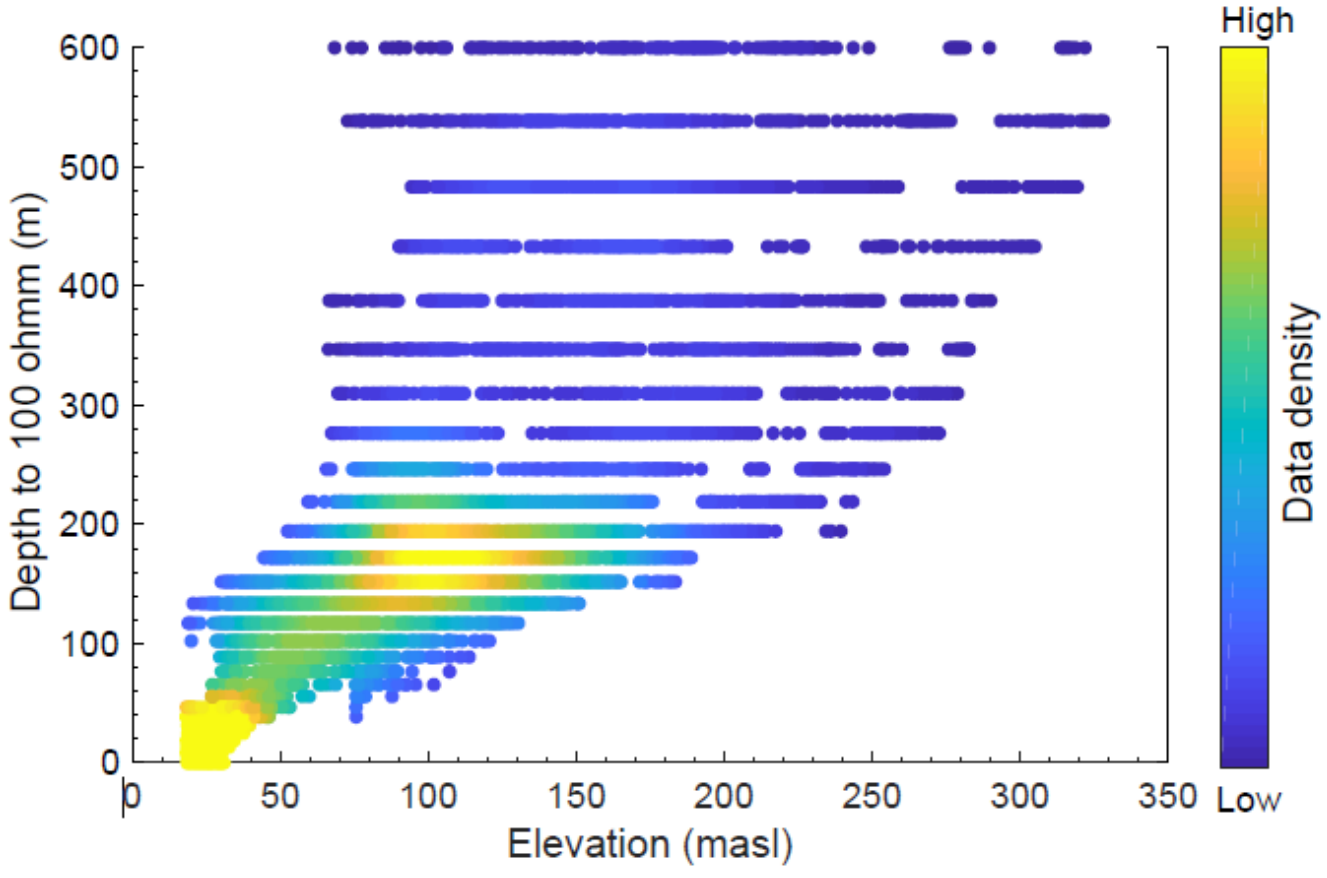

Fig. 9. Elevation versus depth to 100 Ωm brine/permafrost boundary in Fryxell basin. Data density shown in color ramp, where yellow points indicate higher data density and blue points indicate lower data density.

https://doi.org/10.5194/tc-2020-241
Preprint. Discussion started: 25 September 2020

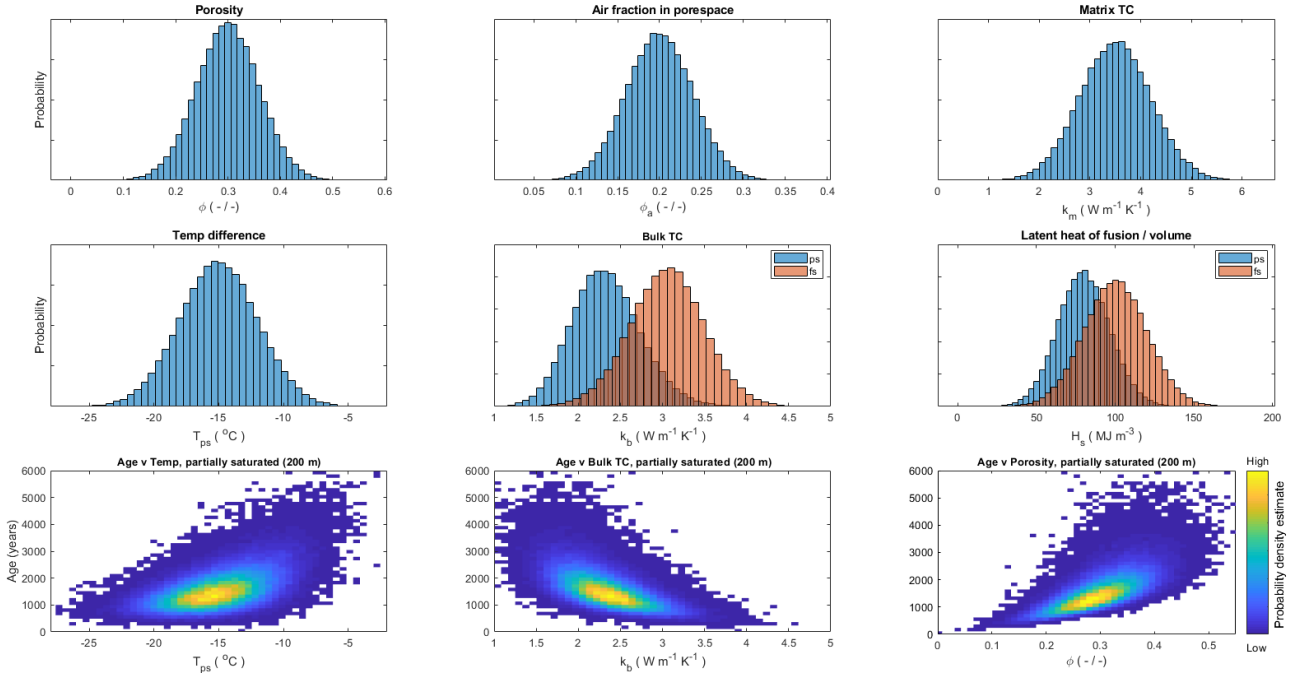

590 Fig. 10. Monte Carlo sensitivity analysis of permafrost age inputs. k_b and H_s include partially saturated (ps) and fully saturated (fs) substrate conditions.

595

600

605

https://doi.org/10.5194/tc-2020-241
Preprint. Discussion started: 25 September 2020

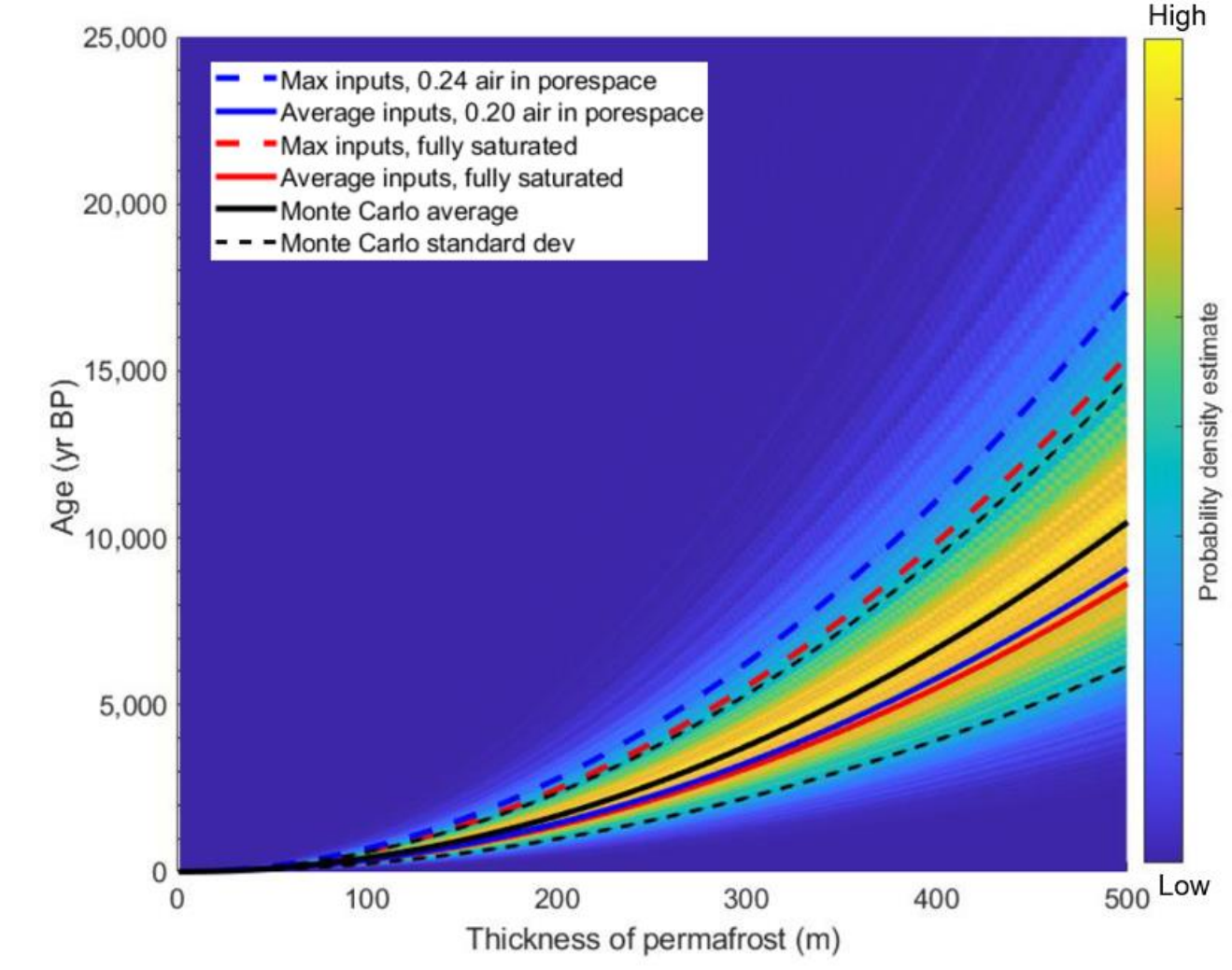

Fig. 11. Monte Carlo age versus elevation probability for 10,000 iterations of Eq. (1) with average inputs and assigned variance. Monte Carlo average result shown as solid black line and one standard deviation as dashed black line. Permafrost ages for average (solid) and maximum inputs (dashed) into Eq. (1), for partially (blue) and completely saturated (red) conditions. Maximum inputs with air fraction in pore of 0.24 space yields maximum possible ages (dashed blue).

https://doi.org/10.5194/tc-2020-241
Preprint. Discussion started: 25 September 2020

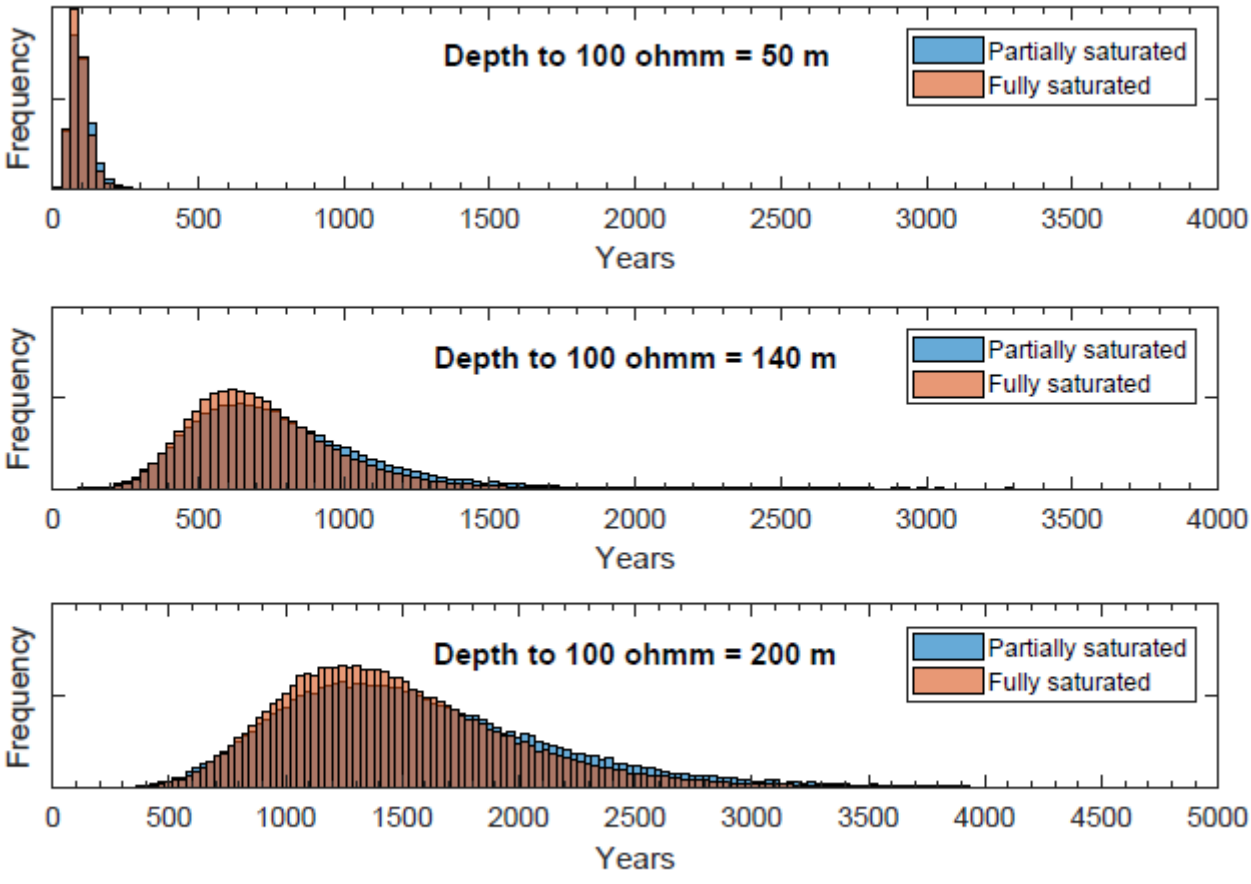

Fig. 12. Age estimates from Monte Carlo analysis as discrete depth to 100 Ωm brine/permafrost boundary. Each panel shows Monte Carlo analysis results for partially saturated (blue) and fully saturated (orange) conditions.

https://doi.org/10.5194/tc-2020-241
Preprint. Discussion started: 25 September 2020

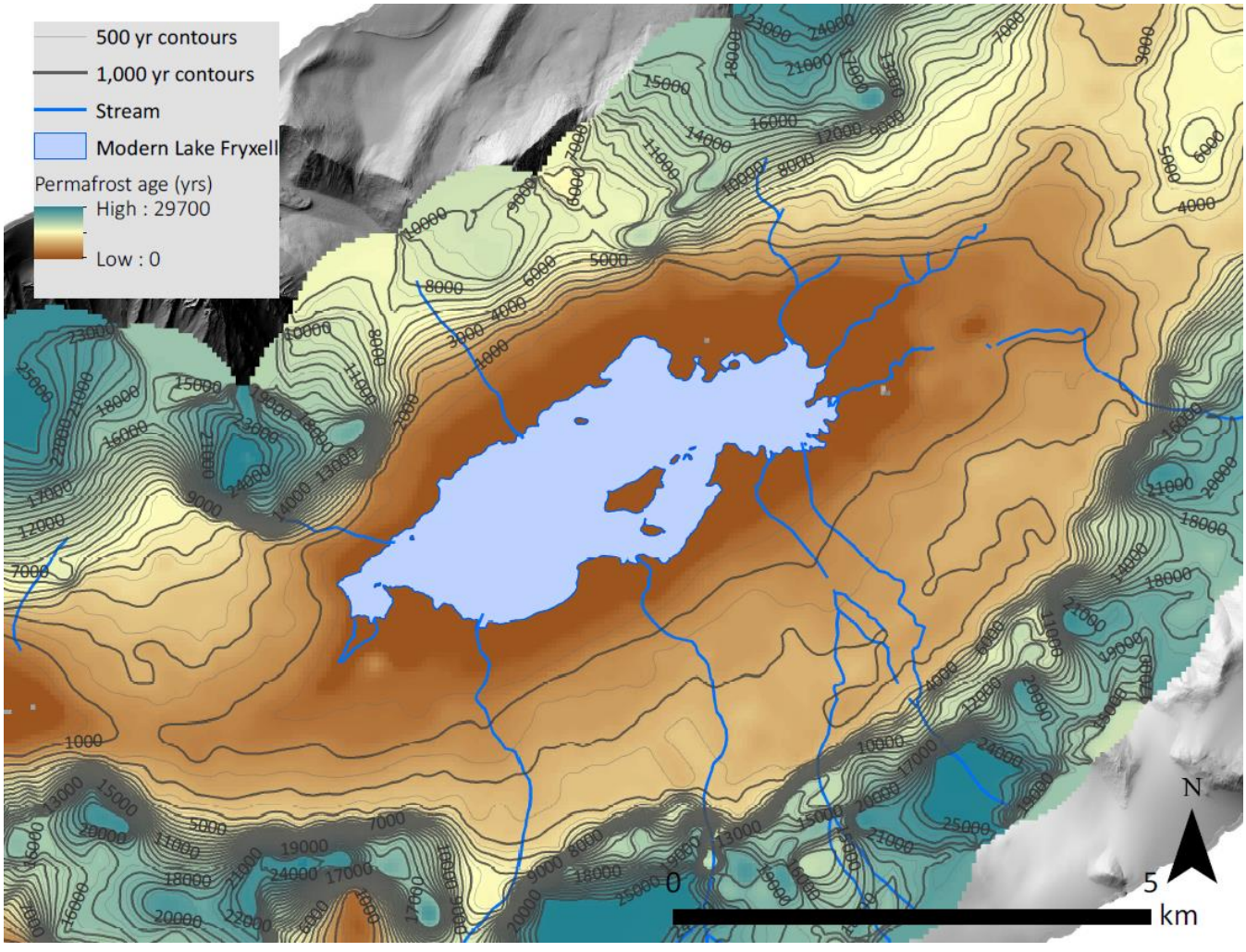

Fig. 13. Maximum permafrost age distribution in Fryxell basin using depth to permafrost-brine boundary (defined as 100 Ωm). Contours represent age of permafrost in years before present, implying recent drainage of GLW during the late Holocene. DEM (1 m resolution) is from 2014-15 LiDAR survey, accessed via OpenTopography (Fountain et al., 2017).

https://doi.org/10.5194/tc-2020-241
Preprint. Discussion started: 25 September 2020

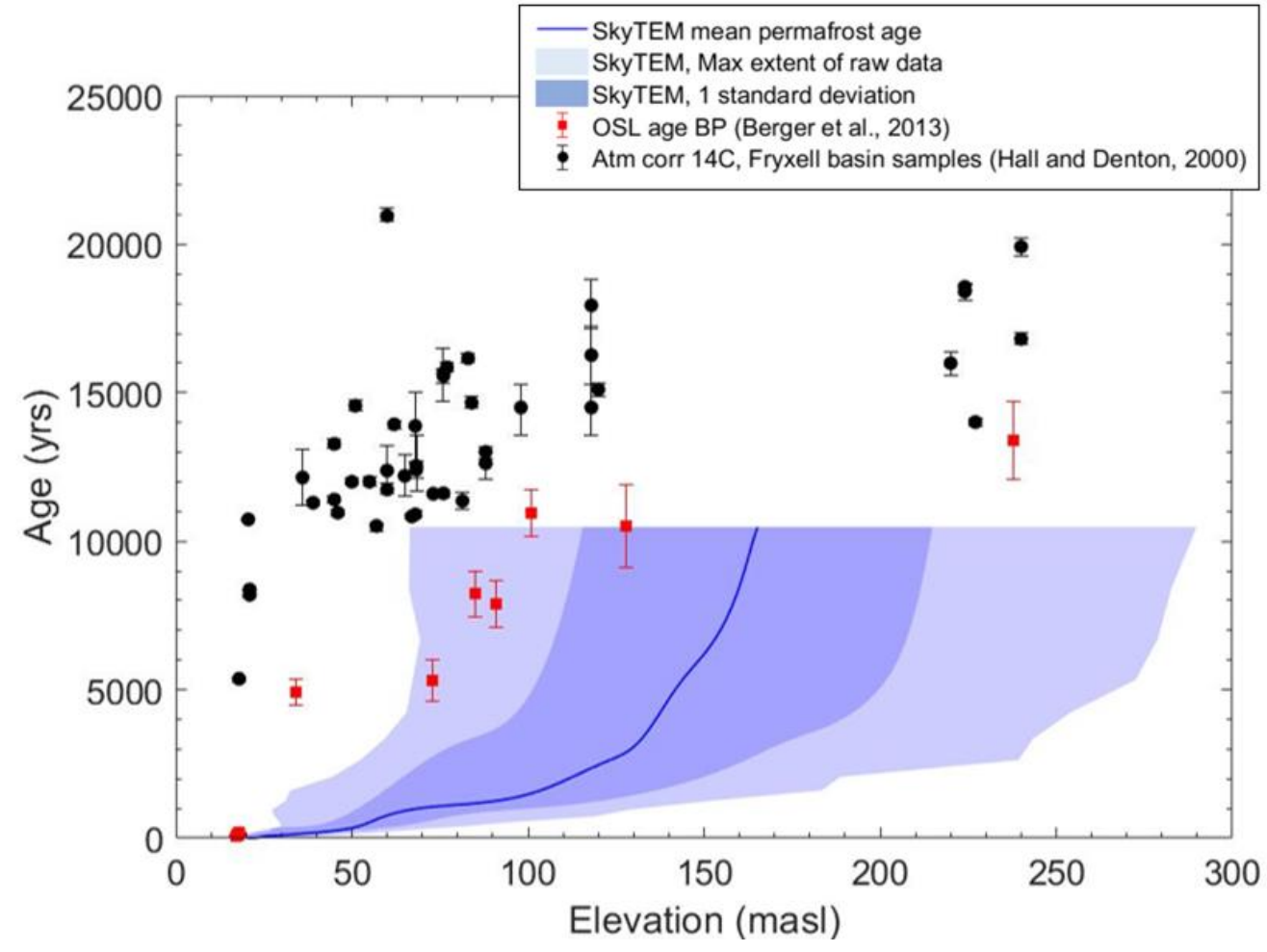

645 Fig. 14. Permafrost ages calculated using SkyTEM resistivity data compared to ^{14}C and OSL ages (Hall and Denton, 2000; Berger et al., 2013). Median permafrost age for each elevation is plotted as solid blue line, one standard deviation is plotted as blue shading, and maximum extent of raw data plotted as light blue shading.

650

https://doi.org/10.5194/tc-2020-241
Preprint. Discussion started: 25 September 2020

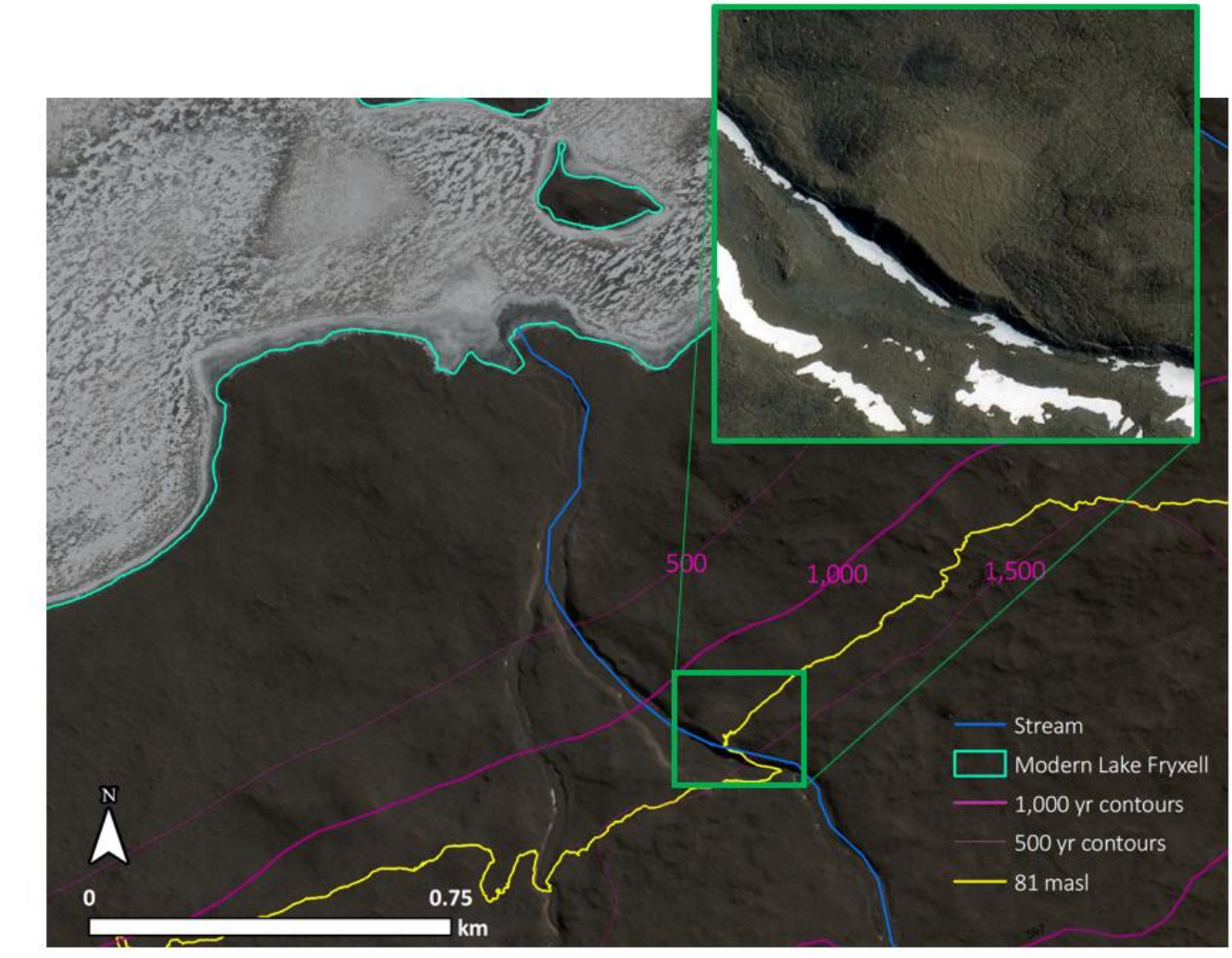

Fig. 15. Maximum permafrost age contours (pink) indicate roughly 1.5 to 1 ka permafrost at 81 masl (yellow). An extremely well-preserved delta on Crescent Stream is located at roughly 81 masl shown in inset map (green). Image © 2017 DigitalGlobe, Inc. and data provide Polar Geospatial Center.

https://doi.org/10.5194/tc-2020-241
Preprint. Discussion started: 25 September 2020


The Cryosphere Discussions

Variable	Mean value	Standard deviation	Max/min value	Description
ϕ	0.30	20 %	0.36	Porosity
ϕ_a	0 / 0.20	20 %	0 / 0.24	Fraction of air in pore space
T_{ps}	-15	20 %	-12	Temperature difference (K)
k_f	2.25	2 %	2.205	TC of fluid (-5 ºC) (W/m K)
k_a	0.0236	2 %	0.0231	TC of air (-10 ºC) (W/m K)
k_m	3.50	20 %	2.80	TC of rock matrix (-5 ºC) (W/m K)
$k_{b,\,fs}$	3.07	-	2.57	Bulk TC (W/m K), fully saturated
$k_{b,\,ps}$	2.33	-	1.73	Bulk TC (W/m K), partially saturated
$H_{s,\,fs}$	100.2	-	120.2	Vol. heat of fusion (MJ/m^3), fully saturated
$H_{s,\,ps}$	80.2	-	91.4	Vol. heat of fusion (MJ/m^3), partially saturated

Table 1. Input values for Monte Carlo analysis. Max/min values column show values within one standard deviation resulting in oldest permafrost ages.